OPEN

Neonatal mice possess two phenotypically and functionally distinct lung-migratory CD103$^+$ dendritic cell populations following respiratory infection

TJ Ruckwardt[1], KM Morabito[1], E Bar-Haim[1,2], D Nair[1] and BS Graham[1]

The CD103$^+$ subset of lung-migratory dendritic cells (DCs) plays an important role in the generation of CD8$^+$ T cell responses following respiratory infection. Here, we demonstrate that the dependence on CD103$^+$ DCs for stimulation of RSV-specific T cells is both epitope and age-dependent. CD103$^+$ DCs in neonatal mice develop two phenotypically and functionally distinct populations following respiratory infection. Neonatal CD103$^+$ DCs expressing low levels of CD103 (CD103lo DCs) and other lineage and maturation markers including costimulatory molecules are phenotypically immature and functionally limited. CD103lo DCs sorted from infected neonates were unable to stimulate cells of the $K^dM2_{82\text{-}90}$ specificity, which are potently stimulated by CD103hi DCs sorted from the same animals. These data suggest that the delayed maturation of CD103$^+$ DCs in the neonate limits the $K^dM2_{82\text{-}90}$-specific response and explain the distinct CD8$^+$ T cell response hierarchy displayed in neonatal mice that differs from the hierarchy seen in adult mice. These findings have implications for the development of early-life vaccines, where the promotion of responses with less age bias may prove advantageous. Alternately, specific approaches may be used to enhance the maturation and function of the CD103lo DC population in neonates to promote more adult-like T cell responses.

INTRODUCTION

Recent studies of the ontogeny of dendritic cells (DCs) have dramatically enhanced our understanding of DC subsets and provided a framework for understanding their functional specialization in both the mouse and human.[1–5] This framework defines two conventional DC (cDC) lineages originating from a common DC precursor (CDP). The first lineage, now referred to as cDC1, encompasses lymph node resident CD8α$^+$ DCs and a non-lymphoid subset of migratory DCs often characterized by surface expression of the integrin alpha E in peripheral tissues (CD103$^+$ DCs). The cDC1 lineage is dependent on the growth factor Fms-like tyrosine kinase 3 ligand (FLT3L) for differentiation, and signaling through the granulocyte macrophage colony-stimulating factor receptor (GM-CSFR) for cell cycle maintenance.[6–8] Several transcription factors are required for development of cDC1, most notably basic leucine zipper transcription factor ATF-like 3 (Batf3) and interferon regulatory factor 8 (IRF8).[9–11] The second lineage of cDCs (cDC2) originating from the CDP consists of lymphoid-resident CD4$^+$ DCs, as well as the non-lymphoid, migratory DC population that expresses the integrin alpha M in the lung (CD11b$^+$ DCs). Their development is also dependent on Flt3L and GM-CSFR, but they are less dependent on GM-CSFR than cDC1.[7,12] Transcription factors governing the development of cDC2 appear more tissue-dependent, with interferon regulatory factor 4 (IRF4) playing a critical role in controlling development, migration, and antigen presentation in CD11b$^+$ DCs.[13–16]

The respiratory tract is a critical barrier tissue, and one of the largest interfaces with the outside environment. Here, the maintenance of lung structure and function must be balanced with tolerance to innocuous antigens and the initiation of

[1]Viral Pathogenesis Laboratory, Vaccine Research Center, National Institute of Allergy and Infectious Diseases, National Institutes of Health, Bethesda, Maryland, USA and [2]Department of Biochemistry and Molecular Genetics, Israel Institute for Biological Research, Ness-Ziona, Israel. Correspondence: TJ Ruckwardt (truckwardt@mail.nih.gov)

Received 23 September 2016; accepted 28 February 2017; published online 5 April 2017. doi:10.1038/mi.2017.28

immune responses to respiratory infection. Following infection, CD103$^+$ DCs and CD11b$^+$ DCs in the lung upregulate CCR7, and carry antigen to the draining mediastinal lymph node (MLN). Antigen is processed and presented in the context of MHC Class I and II. This display of viral epitopes, in conjunction with costimulatory factors and cytokines, allows DCs to orchestrate and regulate adaptive immunity. CD103$^+$ DCs are specialized in the cross-presentation of antigen in MHC Class I, and possess a greater ability to drive Th1 effector responses, making them crucial mediators of immunity to intracellular pathogens.[10,17–21] Conversely, CD11b$^+$ DCs more readily present antigen to CD4$^+$ T cells and counter extracellular pathogens. They take up and process extracellular antigens, and can promote both Th2 and Th17 responses.[14,22,23]

Studies addressing the function and specialization of lung-migratory dendritic cells have primarily focused on adult mice with less understanding of the function, or functional limitations, of these DC subsets in neonates. We have previously shown that neonatal (7day old) CB6F1 mice infected with respiratory syncytial virus (RSV) develop a distinctly different CD8$^+$ T cell epitope hierarchy than infected adult mice. While adults exhibit a strongly immunodominant response to the $K^dM2_{82\text{-}90}$ epitope of RSV, the dominance of this epitope does not occur in neonates, which maintain a codominant response to the $K^dM2_{82\text{-}90}$ epitope and another RSV epitope, $D^bM_{187\text{-}195}$.[24] Coincident with the age-dependent CD8$^+$ T cell response, we have demonstrated both qualitative and quantitative deficiencies in CD103$^+$ DCs and CD11b$^+$ DCs in the MLN of RSV-infected neonatal mice. DCs in the MLN are responsible for the induction of adaptive responses, and have lower functionality and expression of the costimulatory molecules CD80 and CD86. Their limited ability to provide CD28-mediated co-stimulation is related to the co-dominant CD8$^+$ T cell hierarchy established in neonatal mice, as the $K^dM2_{82\text{-}90}$ response appears more dependent on co-stimulation than the response to $D^bM_{187\text{-}195}$.[25]

Here, we demonstrate that the neonatal CD103$^+$ DC subset, which most potently stimulates the CD8$^+$ T cell response, partitions into two phenotypically and functionally distinct populations of cells following respiratory infection which can be identified by the level of expression of CD103. Neonatal CD103lo DCs represent the majority of the CD103$^+$ DC population in naive neonates and during early infection, and express lower levels of lineage-defining markers as well as markers associated with DC maturation. In addition to this phenotypic immaturity, their ability to take up and process antigen is limited, and they demonstrate a striking inability to induce CD8$^+$ T cells of the $K^dM2_{82\text{-}90}$ specificity. Conversely, neonatal CD103hi DCs display a phenotype and functional profile more akin to their adult counterparts, and most notably, induce a T cell profile that mirrors mature adult CD103$^+$ DCs. Infection of neonatal mice with influenza/PR8 resulted in a similar partitioning of CD103$^+$ DCs, indicating that this is a general feature of the neonatal CD103$^+$ DC response and suggests that the events associated with CD103 expression are concurrent with the maturation of neonatal CD103$^+$ DCs. There is much to be understood about mechanisms for the establishment of these two distinct populations of CD103$^+$ DCs in the neonate and the implications, both for the maintenance of tolerance in the setting of the developing lung and for the ability of these cells to effectively induce adaptive responses during neonatal infection or vaccination.

RESULTS

CD103$^+$ DCs from neonatally-infected mice demonstrate an early impairment in the ability to stimulate $K^dM2_{82\text{-}90}$-specific T cells

We have previously shown that neonatal CD103$^+$ DCs isolated from the MLN one day post-infection stimulate a distinct CD8$^+$ T cell profile when compared to adult CD103$^+$ DCs.[25] To further examine this finding, we assessed the ability of the CD103$^+$ and CD11b$^+$ lung-migratory DC subsets to induce CD8$^+$ T cells at different times following RSV infection. We focused on DCs in the lung-draining posterior MLN, the site of CD8$^+$ T cell induction during primary respiratory infection. CD103$^+$ and CD11b$^+$ DCs were sorted from the MLN of RSV-infected adult or neonatal mice on days 1, 2, 3, and 7 post-infection. All neonatal mice were 7days old at the time of infection. Timed-matings and infections were performed such that samples from either adults or neonates at all four times points post-infection were acquired, DCs sorted, and T cell cocultures performed on the same day for optimal comparisons between time points. CD8$^+$ T cells of the $K^dM2_{82\text{-}90}$ and $D^bM_{187\text{-}195}$ specificities were isolated from adult, naive TCR transgenic mice, labeled with CFSE, and co-cultured with sorted DC populations for three days before staining. We determined the frequency of epitope-specific T cells that were stimulated to divide by each DC population using FlowJo proliferation analysis (gating scheme for dendritic cell sorting, and raw data resulting from the coculture of adult and neonatal CD103$^+$ DCs with CD8$^+$ T cells of each specificity are shown in **Supplementary Figure S1** online). Adult CD103$^+$ DCs strongly induced $K^dM2_{82\text{-}90}$-specific T cells at all times points post-infection (**Figure 1a**) and stimulated CD8$^+$ T cell proliferation more potently than CD11b$^+$ DCs (**Figure 1a** vs **Figure 1b**). While stimulating fewer CD8$^+$ T cells, adult CD11b$^+$ DCs stimulated both epitope-specific populations more equally. In contrast, CD103$^+$ DCs isolated from neonatally-infected mice during the first two days post-infection stimulated significantly fewer $K^dM2_{82\text{-}90}$-specific cells than those isolated on or after day 3 post-infection, when the profile of T cell proliferation more closely resembled that of adult CD103$^+$ DCs (**Figure 1c**). Neonatal CD11b$^+$ DCs stimulated RSV-specific CD8$^+$ T cells in a fashion similar to those of adult CD11b$^+$ DCs with lower induction, and less bias toward the $K^dM2_{82\text{-}90}$ response than that of CD103$^+$ DC subset (**Figure 1d**).

Of note, neonatal mice showed an early impairment in their ability to stimulate $K^dM2_{82\text{-}90}$-specific cells when compared to adult CD103$^+$ DCs. This trend is more apparent as a ratio of the percent of CD8$^+$ T cells of each specificity induced to divide (**Figure 1e**). Adult and neonatal CD11b$^+$ DCs show near equal

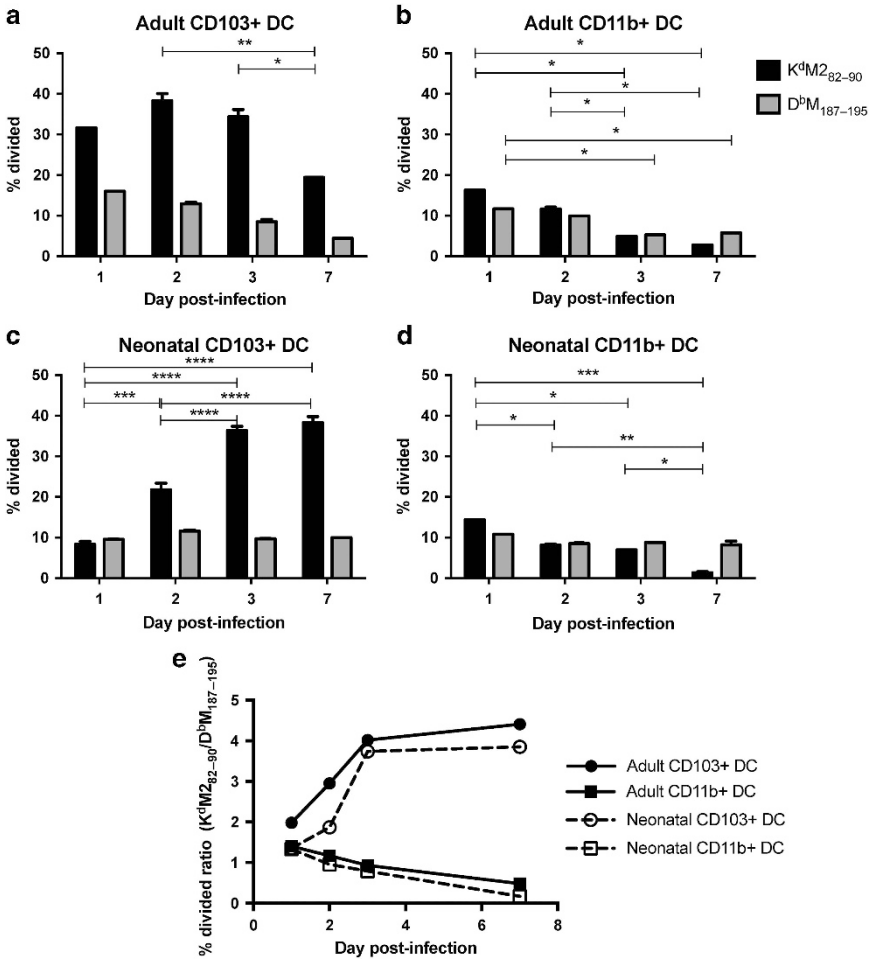

Figure 1 Neonatal CD103$^+$ DCs demonstrate an early impairment in the ability to stimulate K^dM2_{82-90}-specific cells. FACS-sorted adult CD103$^+$ DCs (**a**) adult CD11$^+$ DCs (**b**) neonatal CD103$^+$ DCs (**c**) and neonatal CD11b$^+$ DCs (**d**) from the MLN of RSV-infected mice were cocultured with CFSE-labeled transgenic T cells specific for either the K^dM2_{82-90} or $D^bM_{187-195}$ epitope for three days before surface staining and FACS analysis. The percent of the original TCR transgenic population that was stimulated to divide was calculated by FlowJo software. Data are representative of two complete experiments for each age group, where MLN were pooled to provide two replicates for each time point post-infection on a single harvest day. (**e**) The percent divided ratio for each antigen presenting cell population on each day post-infection was calculated by dividing the percent of K^dM2_{82-90}-specific cells that were induced to proliferate by the percent of $D^bM_{187-195}$-specific cells that were induced to proliferate. Data are representative of two independently performed experiments for each age group with two replicates for each dendritic cell subset and CD8$^+$ T cell response at each day post-infection. * indicates $P<0.05$, **$P<0.01$, ***$P<0.001$, ****$P<0.0001$ by two way ANOVA with Tukey's multiple comparisons test.

(ratio of 1) stimulation of CD8$^+$ T cells of both specificities, with stimulation becoming slightly more skewed toward the $D^bM_{187-195}$ response over the course of infection. The clear bias of adult CD103$^+$ DCs toward induction of the K^dM2_{82-90} response resulted in the stimulation of twice as many K^dM2_{82-90}—specific cells as $D^bM_{187-195}$—specific cells on day 1 post-infection, and an increase in ratio as the infection progressed, further favoring this specificity. While neonatal CD103$^+$ DCs isolated on day 1 post-infection stimulated both specificities equally, the bias of these cells toward K^dM2_{82-90} increased to more closely resemble the response of adults starting at day 3 post-infection. These data demonstrate that each lung-migratory DC subset elicits a distinct profile of epitope-specific CD8$^+$ T cells, and that the ability of these DC subsets to stimulate CD8$^+$ T cells is dependent on both time post-infection and the age at which mice are infected.

CD103$^+$ DCs are dispensable for the induction and maintenance of the K^dM2_{82-90}-specific response in neonatal mice

To assess the global contribution of the CD103$^+$ DC subset to the generation and maintenance of RSV-specific CD8$^+$ T cell responses, we compared CD8$^+$ T cell responses in neonatal and adult Batf3$^{-/-}$ CB6F1 mice to those of wild-type mice after RSV infection. Batf3$^{-/-}$ mice lack cDC1, and have been shown to exhibit reduced CD8$^+$ T cell responses to multiple pathogens, confirming the importance of this lineage to the development of CD8$^+$ T cell responses.[10,26,27] CD8$^+$ T cell responses were compared at day 7, the peak of the response in infected mice. Batf3$^{-/-}$ neonatal and adult mice had a significantly lower frequency of CD8$^+$ T cells in the lungs overall (**Supplementary Figure S2A**), but not in the MLN (**Supplementary Figure S2B**). While the lungs of adult Batf3$^{-/-}$ mice had a trend toward a

lower number of $CD8^+$ T cells than wild-type mice (**Supplementary Figure S2C**), the $CD8^+$ T cell count in the MLN of adult infected $Batf3^{-/-}$ was significantly increased as compared to wild-type mice (**Supplementary Figure S2D**). The number of $CD8^+$ T cells was less affected in Batf3-deficient neonates, with no significant difference in the lung or MLN in the absence of $CD103^+$ DCs.

RSV epitope-specific $CD8^+$ T cell responses were altered considerably in $Batf3^{-/-}$ mice. $Batf3^{-/-}$ neonatal and adult mice had a significant reduction in the number and frequency of the $D^bM_{187\text{-}195}$-specific response (**Figure 2a** and **c**, respectively). Responses to this epitope were 3.8-fold reduced in Batf3-deficient adult mice, and reduced by 1.6-fold in neonates. Similar significant reductions in the number and frequency of the $D^bM_{187\text{-}195}$-specific response were observed in the MLN (**Supplementary Figures S2E and S2G**). The $K^dM2_{82\text{-}90}$-specific response in adult mice was similarly dependent on $CD103^+$ DCs in the lung; the frequency (**Figure 2b**) and the number (**Figure 2d**) of cells responding to this epitope were significantly lower in $Batf3^{-/-}$ adults than in wild-type controls. Unexpectedly, the absence of $CD103^+$ DCs in neonates resulted in a significant increase in the frequency (**Figure 2b**) and number (**Figure 2d**) of $K^dM2_{82\text{-}90}$-specific cells in the lung.

We have previously demonstrated that the absence of the $D^bM_{187\text{-}195}$ epitope leads to an increase in the $K^dM2_{82\text{-}90}$-specific response in the context of primary RSV infection.[28] We hypothesized that the increase in the $K^dM2_{82\text{-}90}$-specific response in $Batf3^{-/-}$ neonatal mice was due to a reduction in competition from the $D^bM_{187\text{-}195}$ response, which was significantly lowered by Batf3-deficiency. To test this hypothesis, neonatal $Batf3^{-/-}$ mice were infected with RSV-N191S, a virus with a mutation in the D^b-binding anchor residue of the $M_{187\text{-}195}$ peptide that completely abrogates the T cell response to $D^bM_{187\text{-}195}$.[28] Upon infection with this viral mutant, $K^dM2_{82\text{-}90}$–specific responses were found to be unchanged by the absence of $CD103^+$ DCs, indicating that the increase in the $K^dM2_{82\text{-}90}$ response in $Batf3^{-/-}$ neonates infected with wild-type RSV was caused, at least in part, by a decrease in competition from the $D^bM_{187\text{-}195}$-specific response (**Supplementary Figure S3**).

Our findings demonstrate that the requirement of $CD103^+$ DCs for the induction and maintenance of $CD8^+$ T cell responses is age and epitope-dependent. Both $CD8^+$ T cell responses in adult mice are heavily reliant on $CD103^+$ DCs and significantly diminished in their absence. While the $D^bM_{187\text{-}195}$-specific response of neonates similarly relies on $CD103^+$ DC, the $K^dM2_{82\text{-}90}$ –specific response in neonatal mice does not, indicating that the $CD103^+$ DC subset is entirely dispensable for the generation of this response in neonatal, but not adult mice.

Two distinct populations of lung-migratory $CD103^+$ DCs are present in intranasally-infected neonatal mice

On the basis of age-dependency in the requirement of $CD103^+$ DCs for the induction of $CD8^+$ T cell responses, we further

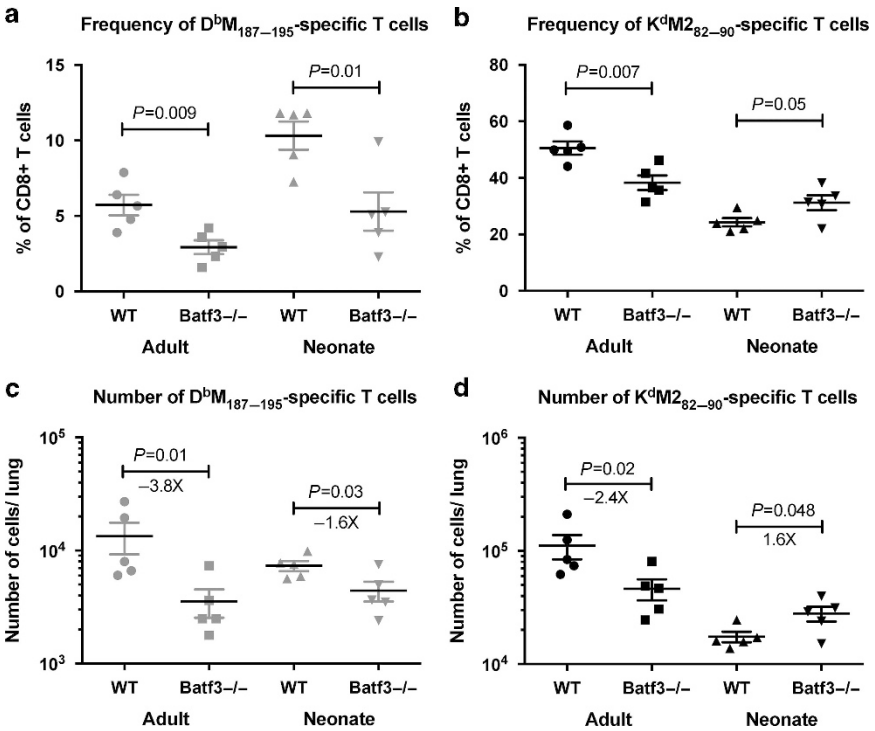

Figure 2 $CD103^+$ DCs are dispensable for the induction and maintenance of the $K^dM2_{82\text{-}90}$-specific $CD8^+$ T cell response in neonates. Wild-type and $Batf3^{-/-}$ adult and neonatal mice were infected intranasally with RSV. Seven days post-infection, the frequency and number of $D^bM_{187\text{-}195}$-specific (**a** and **c**, respectively) and $K^dM2_{82\text{-}90}$-specific (**b** and **d**) cells in the lung were determined. Data are representative of 3 independent experiments with 5–8 mice per group. *P* values indicated are from a t-test between wild-type and $Batf3^{-/-}$ mice of the same age.

explored differences between neonatal and adult CD103$^+$ DCs. We first compared lung-migratory DC populations in naive adults and neonates (**Figure 3a**). In addition to possessing a lower frequency of CD11b$^+$ DCs as we have previously described,[25] the CD103$^+$ DC subset in neonatal mice was characterized by lower expression of the lineage-defining surface marker CD103. Naive adult CD103$^+$ DC also presented higher expression levels of CD11b than those of neonates. Throughout primary infection, adult CD103$^+$ DCs form a single population of cells with high expression of CD103 and low, but observable expression of CD11b (**Figure 3b**). In contrast, neonatal CD103$^+$ DCs segregate into two distinct populations, one reminiscent of CD103$^+$ DCs found in naive neonatal mice that express low levels of CD103 (CD103lo DCs, **Figure 3b**). A second population with increased expression of both CD103 and CD11b appears one day post-infection, and forms a second population within the subset through the remainder of primary RSV infection (CD103hi DCs). The partitioning of the neonatal CD103$^+$ DC subset into two distinct populations during respiratory infection occurred in a similar fashion during infection of neonatal mice with influenza/PR8 (**Supplementary Figure S4**), indicating that this is a common feature of the neonatal CD103$^+$ DC subset following respiratory infection.

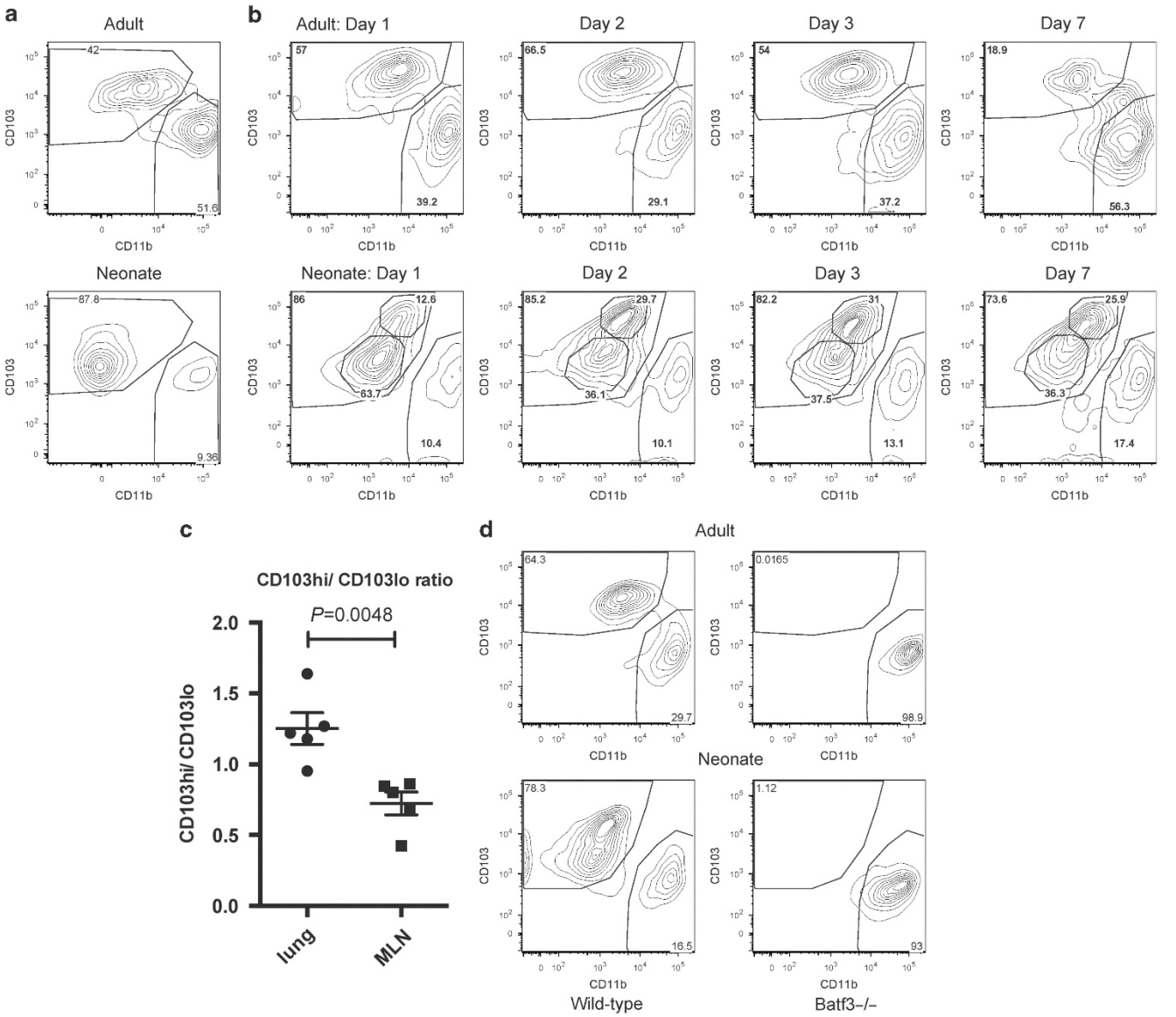

Figure 3 Neonatal mice infected with RSV possess two distinct populations of Batf3-dependent CD103$^+$ DCs. (**a**) Lung-migratory DC populations in the MLN of naive adult and neonatal mice. (**b**) Lung-migratory DC populations in the MLN of RSV-infected adult and neonatal mice on days 1, 2, 3 and 7 post-infection. Data are representative of two independent experiments with 2–3 samples of pooled lymph nodes each. (**c**) CD103hi DC/CD103lo DC ratio in the lung and MLN of neonatal mice two days post-RSV infection. Data are representative of two independent experiments, each containing 3–4 biological replicates of pooled lymph nodes and lungs. Groups were compared using a *t* test. (**d**) DC populations in the MLN of wild-type and Batf3$^{-/-}$ adults and neonates 2 days post-RSV infection confirm the dependence of both populations on the transcription factor Batf3. Data are representative of two independent experiments with 2–3 biological replicates from each strain of mice.

We next compared the composition of CD103lo and CD103hi DCs in the lungs and MLN of neonatal mice. On day 2 post-infection, the ratio of CD103hi DCs/CD103lo DCs in the lungs was significantly higher than in the MLN, indicating an enrichment for CD103lo DCs in the MLN ($P = 0.0048$, **Figure 3c**). To ensure that both populations of the CD103$^+$ DC subset in neonates represent bona fide, Batf-dependent CD103$^+$ lung-migratory DCs, we examined dendritic cells in the MLN two days post-infection in wild-type and Batf3$^{-/-}$ adult and neonatal mice. As expected, adult Batf3$^{-/-}$ mice entirely lacked CD103$^+$ DCs (**Figure 3d**). Neonatal mice were found to lack both CD103lo and CD103hi DC populations within the CD103$^+$ DC subset, confirming their common, Batf3-dependent origin.

GM-CSF, IL-3, and TGFβ have each been demonstrated to promote the expression of CD103 on dendritic cells.[29] To investigate differences in the lung environment that may limit CD103 expression, we measured the levels of these cytokines in lung supernatants of adults and neonates on day 0 (naive adult and 7 day-old mice), and on days 1, 2, 3, and 7 post-infection. Higher expression of GM-CSF was found in the lungs of naive adults than naive neonates. The expression level in adults was also significantly higher on days 1, 3, and 7 post-infection (**Figure 4a**). Conversely, while relatively low overall, expression of IL-3 tended to be higher in neonatal mice, and was significantly higher in neonates on days 1, 2, and 7 post-infection (**Figure 4b**). TGFβ levels were significantly higher in naive neonates, and at every time point post-infection (**Figure 4c**). These data reflect differences in the adult and neonatal lung environment that may play a role in the development and function of lung-migratory dendritic cells. In particular, low steady-state expression of GM-CSF in neonates may play a role in limiting the development of CD103$^+$ DC during early life.

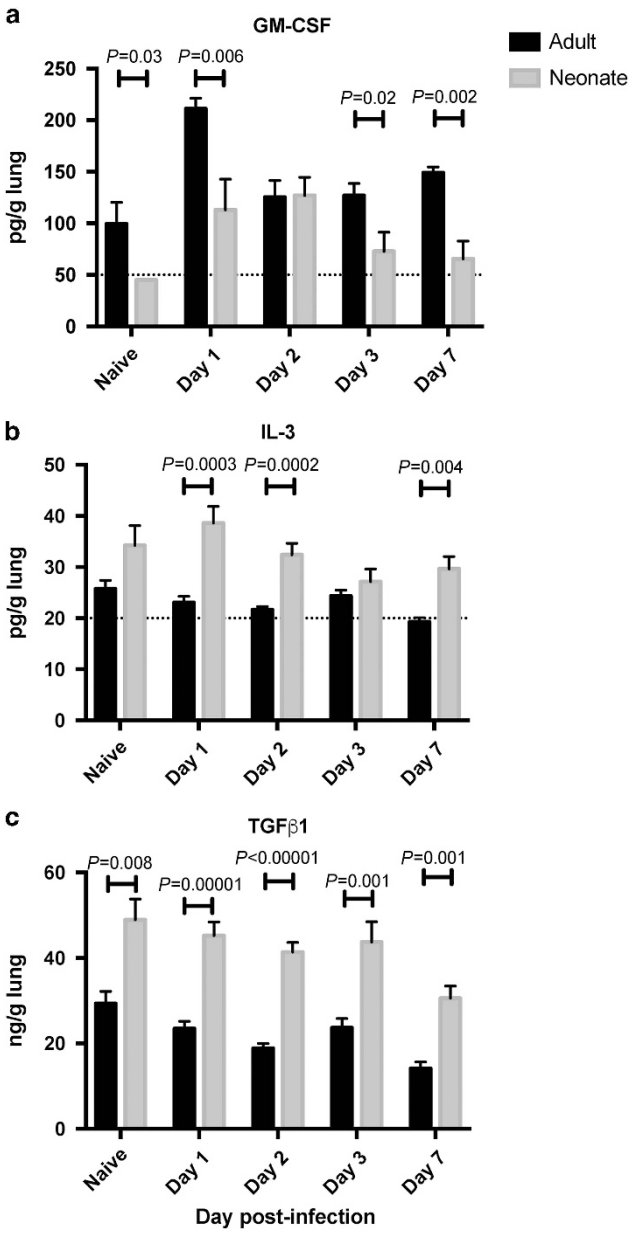

Figure 4 (**a**) GM-CSF, (**b**) IL-3 and (**c**) TGFβ expression levels in the lungs of naive neonatal (7 day-old) and adult mice, and during acute RSV infection. The single left lobe of naive and infected mice was quick-frozen at the indicated time-point. Post-thawing, lungs were ground on a GentleMACS, and lung supernatants clarified by centrifugation before cytokine analysis. Data shown are from an experiment using 5 (Naive, Day 7), or 10 (Days 1, 2, and 3) mice per group. For statistical analysis, a Student's t-test was performed comparing samples from each indicated time point. The dashed line indicates the limit of detection for GM-CSF and IL-3, where some samples had undetectable levels of cytokine.

Neonatal CD103lo and CD103hi DCs are phenotypically distinct

We compared the expression of phenotypic markers between the two CD103$^+$ DC populations in neonates, and to adult CD103$^+$ DCs. Two days after infection, neonatal CD103$^+$ DCs from the MLN of neonates and adults were gated as indicated in **Figure 3b**. Neonatal CD103lo DCs were compared to CD103hi DCs on a forward vs side scatter plot, revealing that the CD103hi DC population is of greater size and complexity than CD103lo DCs (**Figure 5a**). The scatter characteristics of the CD103hi DC population were more comparable to those of adult CD103$^+$ DCs (**Figure 5b**). In addition to CD103, neonatal CD103lo DCs were found to exhibit lower expression of other lineage-defining markers including MHC Class II (I-A^b), CD11b, and CD11c (**Figure 5c**). The expression of these markers on neonatal CD103hi DCs were indistinguishable from adult CD103$^+$ DCs with the exception of CD11b, which was expressed in lower levels on neonatal CD103hi DCs than on adult CD103$^+$ DCs.

We have previously shown that neonatal CD103$^+$ DCs have lower surface expression of the co-stimulatory molecules CD80 and CD86 than adult CD103$^+$ DC.[25] We compared the expression of these markers on neonatal CD103lo and CD103hi DCs, and adult CD103$^+$ DCs from the MLN. Neonatal CD103hi DCs were found to have significantly higher expression of both co-stimulatory molecules than CD103lo DCs in the same mouse (**Figure 5d** and **e**). While their expression is higher than on CD103lo DCs, CD103hi DCs still express significantly lower levels than adult CD103$^+$ DCs,

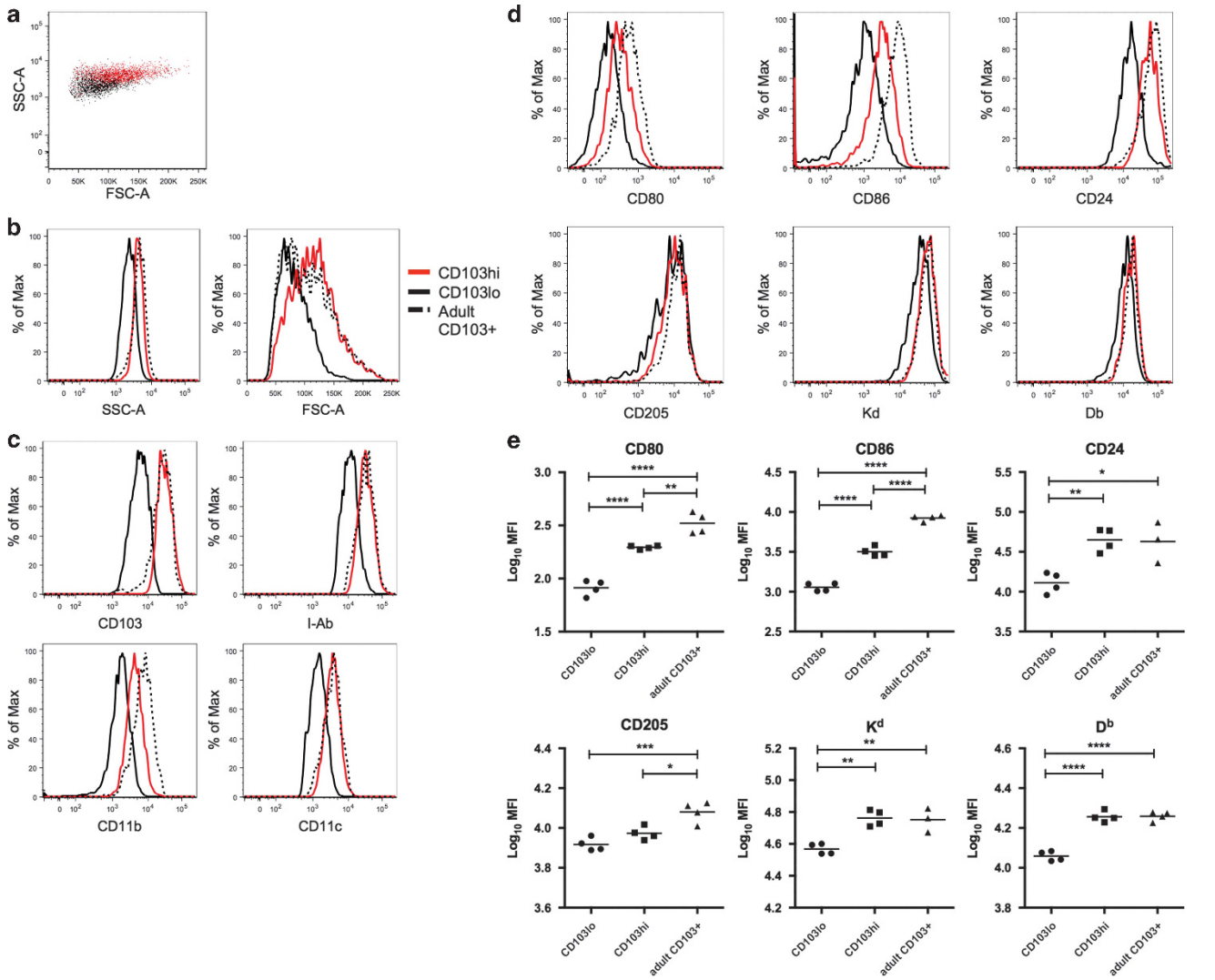

Figure 5 Phenotypic differences between CD103hi and CD103lo DC populations in the MLN of neonatally-infected mice. MLN were harvested 2 days post-infection from mice infected at 7 days of age or as adults. (**a**) FSC vs SSC plot demonstrates size and complexity differences between neonatal CD103lo DCs (black) and CD103hi DCs (red). (**b**) Histograms of side and forward scatter comparing the neonatal CD103lo (black), CD103hi (red), and adult CD103$^+$ (hatched) DC populations. (**c**) Surface staining was performed to measure expression of CD103, I-Ab, CD11b, and CD11c lineage-defining markers on neonatal CD103lo, CD103hi, and adult CD103$^+$ DC populations. (**d**) Representative histograms comparing expression of CD80, CD86, CD24, CD205, K^d, and D^b on neonatal CD103hi and CD103lo DCs and adult CD103$^+$ DCs (**e**) Background (fluorescence minus one)-subtracted median fluorescence intensity (MFI) is presented for CD80, CD86, CD24, CD205, and the MHC Class I molecules K^d and D^b on neonatal CD103lo, CD103hi, and adult CD103$^+$ DCs. Data are representative of two independent experiments with 3–4 mice per group. *indicates $P<0.05$, **$P<0.01$, ***$P<0.001$, ***$P<0.0001$ by one-way ANOVA with Tukey's multiple comparisons test.

indicating that CD103hi DCs are not equivalent to the adult CD103$^+$ DCs despite having many common phenotypic features with them. We further examined expression of the co-stimulatory molecule CD24 and CD205 (DEC205), an endocytic receptor important for the recognition of apoptotic or necrotic cells and the MHC K^d and D^b Class I molecules. Neonatal CD103lo DCs had significantly lower expression of CD24 than CD103hi and adult CD103$^+$ DCs, while CD205 expression on CD103lo and CD103hi DCs were similar and significantly reduced compared to adult CD103$^+$ DCs. Neonatal CD103lo DCs also had significantly lower expression of both MHC Class I molecules than both CD103hi and adult CD103$^+$ DC, which expressed equivalent levels of each (**Figure 5d** and **e**). Overall, neonatal CD103lo DCs present a less mature phenotype than CD103hi DCs, with lower surface expression of several proteins important for DC function.

Given the significant phenotypic differences observed within the CD103$^+$ DC subset, neonatal CD11b$^+$ DCs were compared with adult CD11b$^+$ DCs. Neonatal CD11b$^+$ DCs had a similar forward and side scatter profile to adult CD11b$^+$ DCs, in addition to similar expression of lineage-defining markers (**Supplementary Figure S5A**). As expected based on our previous results, neonatal CD11b$^+$ DCs had significantly lower expression of the costimulatory molecules CD80 and CD86, but their expression of CD24, CD205, and the Class I molecules K^d and D^b were indistinguishable from those

of adult CD11b$^+$ DCs (**Supplementary Figure S5B**). While CD11b$^+$ DCs in the neonate have lower CD80 and CD86 expression and are significantly lower in number than adult CD11b$^+$ DCs,[25] expression of other lineage-defining and functional markers is similar.

Neonatal CD103lo DCs are functionally limited and demonstrate an inability to stimulate the $K^dM2_{82\text{-}90}$-specific response

To compare the ability of neonatal CD103lo and CD103hi DCs to take up and transport soluble protein to the MLN, ovalbumin protein conjugated to Alexa647 (Ova Ax647) was co-administered intranasally at the time of RSV infection. Two days post-infection, the frequency of Alexa647$^+$ DCs in the MLN was measured as compared to mice infected with RSV only. Approximately 60% of the neonatal CD103hi DCs in the MLN of mice that received Ova Ax647 were Alexa647$^+$, significantly more than CD103lo DCs, of which only 15% were positive (**Figure 6a** and **c**). Despite significant functional improvement over the CD103lo DC population, CD103hi DCs were still significantly less able to transport soluble antigen than adult CD103$^+$ DCs (**Figure 6b** and **c**). Next, we assessed each DC population's ability to process antigen by co-administration of DQ ovalbumin (Ova DQ) at the time of infection. This protein, heavily labeled with BODIPY dyes, is non-fluorescent but yields brightly fluorescent, dye-labeled peptides when processed. Two days post-infection, neonatal CD103hi DCs in the MLN were more than five times more likely to have processed Ova DQ than CD103lo DCs in the same mice (6.73 vs 38.3%, **Figure 6d** and **f**). Again, the function of neonatal CD103hi DCs was significantly lower than adult CD103$^+$ DCs, which were 50% Ova-DQ$^+$ (**Figure 6e** and **f**). These data demonstrate that while more neonatal CD103hi DCs take up and process antigen than neonatal CD103lo DCs, adult CD103$^+$ DC remain significantly more effective at antigen uptake and processing than either neonatal population.

Finally, we evaluated the ability of neonatal CD103lo and CD103hi DC populations to stimulate RSV-specific CD8$^+$ T cells. Both DC populations were sorted from the MLN of neonates two days post-infection and cocultured with CD8$^+$ T cells specific for $K^dM2_{82\text{-}90}$ or $D^bM_{187\text{-}195}$. Control samples cultured with naive CB6F1 splenocytes with no peptide, or with 10^{-6}M of specific peptide served as negative and positive controls, respectively. Neonatal CD103hi DCs robustly stimulated proliferation of $K^dM2_{82\text{-}90}$-specific cells, resulting in proliferation of nearly half of the original population (**Figure 7**) and were able to stimulate proliferation in ~15% of $D^bM_{187\text{-}195}$-specific cells. This profile of CD8$^+$ T cell induction by neonatal CD103hi DCs is similar to the profile of induction by adult CD103$^+$ DCs, with a strong bias toward the $K^dM2_{82\text{-}90}$ response (**Supplementary Figure S1B**). In striking contrast, CD103lo DCs sorted from the same neonatal mice displayed an inability to stimulate $K^dM2_{82\text{-}90}$-specific cells, while retaining the ability to stimulate approximately half as many $D^bM_{187\text{-}195}$-specific cells as neonatal CD103hi DCs (**Figure 7**). To rule out a limitation in the ability of CD103lo DC to present the $M2_{82\text{-}90}$ peptide in the context of H2-K^d, we pulsed both CD103hi and CD103lo populations with saturating peptide (10^{-6}M) for one hour before washing and co-culturing with $K^dM2_{82\text{-}90}$-specific CD8$^+$ T cells. Both populations equally presented the exogenously provided $M2_{82\text{-}90}$ peptide and induced maximum proliferation of the T cells (**Supplementary Figure S6**). When pulsed with a lower concentration of $M2_{82\text{-}90}$ peptide (10^{-8}M), CD103lo DC tended to stimulate fewer CD8$^+$ T cells than CD103hi DC, though we cannot preclude the potential contribution of differences in endogenously presented peptide by the two subsets sorted from RSV-infected mice. These data demonstrate that the neonatal CD103lo DC population has a $D^bM_{187\text{-}195}$-biased induction profile, further differentiating the functional profile of the CD103lo and CD103hi DC populations.

DISCUSSION

CD103$^+$ DCs are specialized cross-presenters of viral antigens.[13] In accordance with the observations of several others,[10,26,30] we demonstrate here that the lung-migratory CD103$^+$ DC subset is the most potent stimulator of the anti-viral CD8$^+$ T cell response following respiratory infection. While we have shown direct infection of lung-migratory dendritic cells to be relatively limited ($<1\%$,[25]), these results represent the combined abilities of these dendritic cells to directly present and cross-present antigen. We have previously shown that CD103$^+$ DCs outnumber CD11b$^+$ DCs in the MLN by a factor of nearly 2:1 in adults and 6:1 in neonates following RSV infection,[25] indicating that we are likely underestimating the difference in abilities of these lung-migratory DC subsets to stimulate CD8$^+$ T cells. Despite these differences, CD11b$^+$ dendritic cells are capable of eliciting anti-viral CD8$^+$ T cells in Batf3$^{-/-}$ mice, and we routinely measure stimulation of RSV-specific responses by this subset in adults and neonates (**Figure 1b** and **d**, respectively). Of note, the major factor accounting for the difference in potency between DC subsets is the strong induction of the $K^dM2_{82\text{-}90}$-specific response by adult CD103$^+$ DCs. The early neonatal CD103$^+$ DC subset does not possess this $K^dM2_{82\text{-}90}$-bias, and we demonstrate here that the $K^dM2_{82\text{-}90}$-specific response in neonates is completely independent of CD103$^+$ DCs, in contrast to adults. The limited ability of neonatal CD103$^+$ DCs to support the induction of the $K^dM2_{82\text{-}90}$-specific response likely belies the distinct CD8$^+$ T cell hierarchy found following RSV infection of neonatal mice.[24]

Our data demonstrate that the induction of CD8$^+$ T cell responses is not only APC and epitope-dependent, but also age-dependent. This work additionally cautions against using responses to a single epitope to generalize about the requirements for all CD8$^+$ T cells. Our previous work has shown significant functional differences between the high-affinity $D^bM_{187\text{-}195}$ – specific response and the dominant, yet lower-affinity $K^dM2_{82\text{-}90}$-specific response.[24,28,31] Further understanding of the rules governing the elicitation of these distinct anti-viral responses may offer insight into the unique limitations of neonatal innate and adaptive immunity.

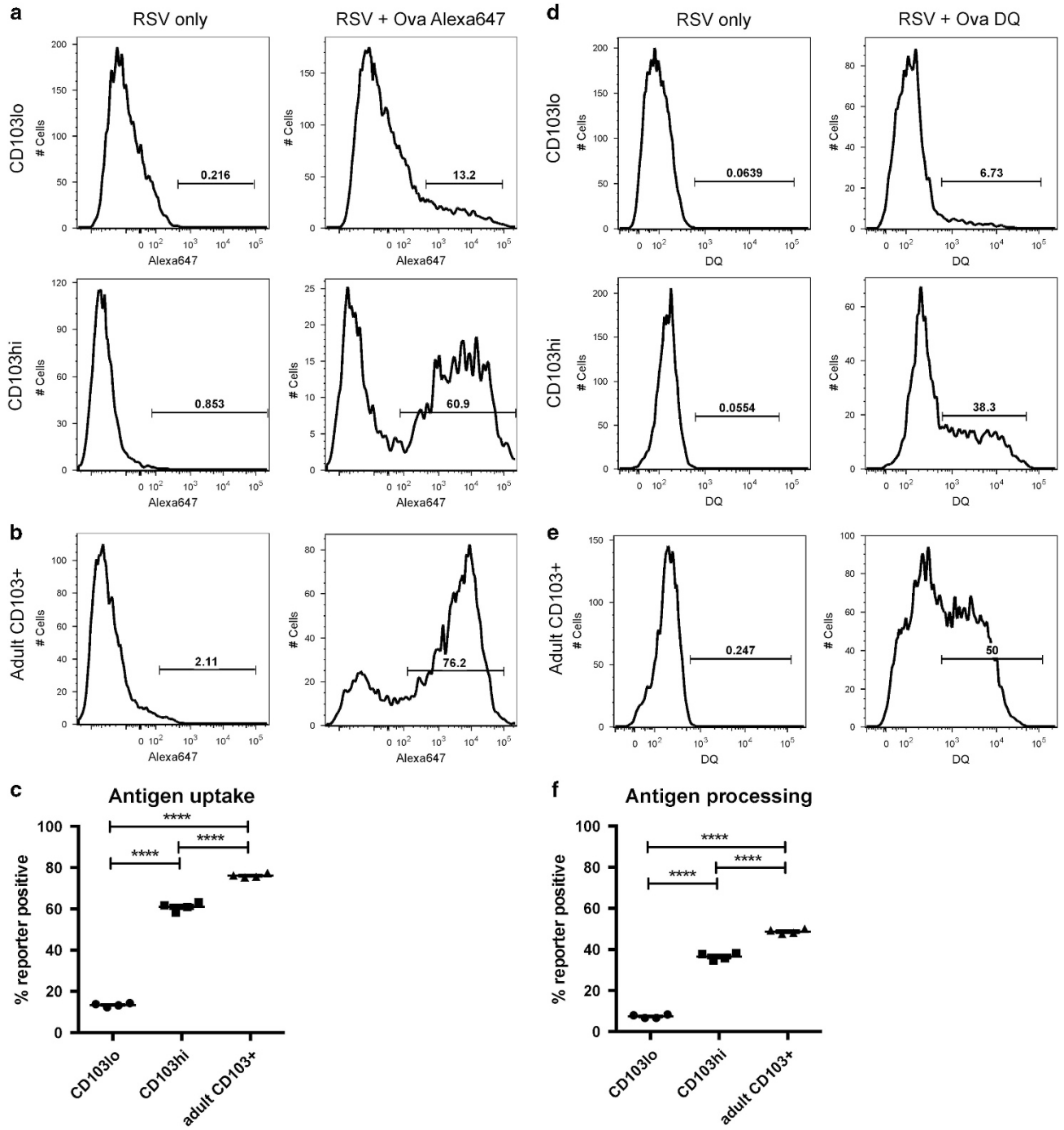

Figure 6 Neonatal CD103$^+$ DCs are deficient in antigen uptake and processing. Labeled ovalbumin proteins (Ova Ax647 or Ova DQ) were co-administered at the time of RSV infection, and fluorochrome positive DCs were measured in the MLN 2 days post-infection. (**a**) Alexa647$^+$ neonatal CD103lo and CD103hi DCs were measured in mice that received co-administered Ova Alexa647 at the time of RSV infection. (**b**) Alexa647$^+$ CD103$^+$ DCs measured in the MLN of adult mice two days post-infection. (**c**) A comparison of antigen uptake by neonatal CD103lo and CD103hi DCs, and adult CD103$^+$ DCs. (**d**) DQ$^+$ neonatal CD103lo and CD103hi DCs were measured in mice that received co-administered Ova DQ. (**e**) DQ$^+$ CD103$^+$ DC in the MLN of adult mice two days post-infection. (**f**) A comparison of antigen processing by neonatal CD103lo and CD103hi DCs, and adult CD103$^+$ DCs. Data are representative of two independent experiments with at least two biological replicates of pooled lymph nodes each. ****indicates $P<0.0001$ by one-way ANOVA with Tukey's multiple comparisons test.

The absence of both the CD103hi and CD103lo DC populations in RSV-infected Batf3$^{-/-}$ neonatal mice confirms the common cDC1 lineage of these populations. In naive neonatal mice, CD103$^+$ DCs assume a nearly uniform CD103lo phenotype. Rather than present a maturation gradient following infection, neonatal CD103$^+$ DCs appear to partition

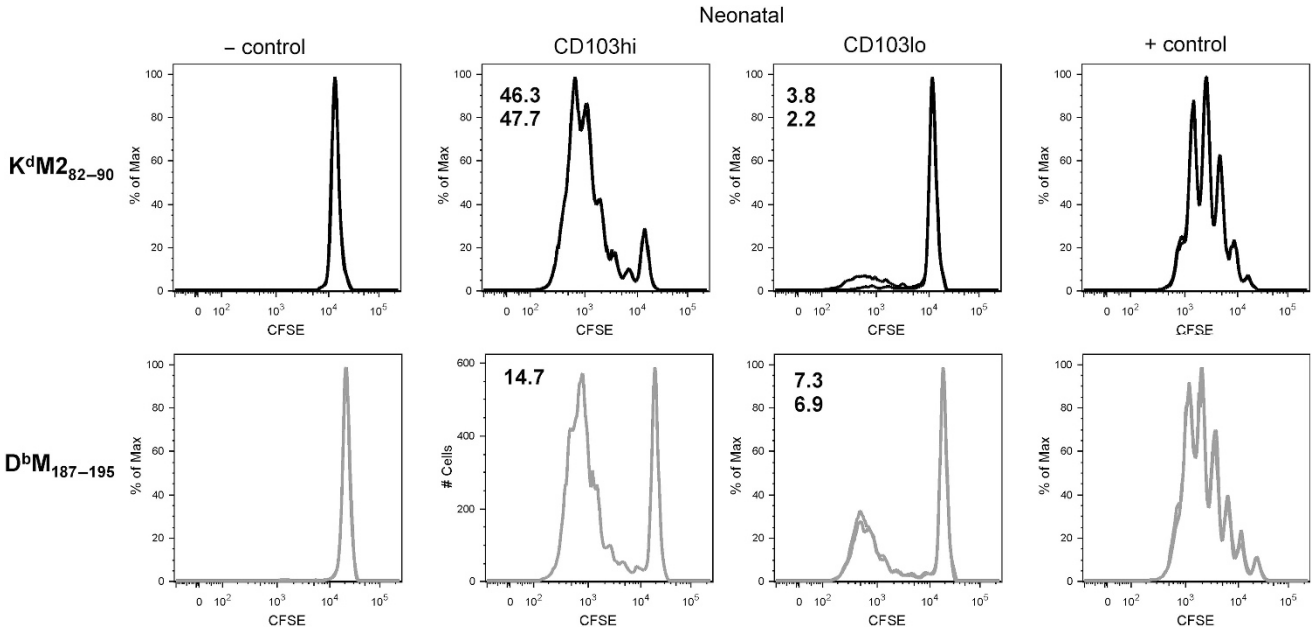

Figure 7 Neonatal CD103lo DC cannot stimulate $K^dM2_{82\text{-}90}$-specific $CD8^+$ T cells. CD103hi and CD103lo DCs were sorted from the MLN two days post-RSV infection of neonatal mice and cocultured with CFSE-labeled $K^dM2_{82\text{-}90}$ or $D^bM_{187\text{-}195}$-specific $CD8^+$ T cells. The percent of transgenic cells induced to proliferate after three days in culture was calculated using Flowjo software. Splenocytes with no peptide, or with 10^{-6}M specific peptide served as antigen presenting cells for the negative and positive controls, respectively. Data are representative of two independent experiments with duplicate samples for each specificity stimulated by CD103lo and CD103hi DCs acquired by FACS-sorting from pooled MLN samples.

into either more mature CD103hi DCs or remain immature CD103lo DCs. These immature, underdeveloped CD103lo DCs in the MLN display lower expression of lineage-defining markers, which may be partially due to their smaller size/surface area. Significantly lower expression of K^d, D^b, and I-A^b may be indicative of lower antigen processing and presentation via MHC Class I and Class II. Coupled with low expression of the costimulatory molecules CD80, CD86, and CD24, neonatal CD103lo DCs are unlikely to productively stimulate anti-pathogen T cell responses in the lung-draining MLN. This idea is further supported by the coculture experiments in which CD103lo DCs demonstrate a complete deficiency in stimulating $K^dM2_{82\text{-}90}$-specific $CD8^+$ T cells, and reduction in the ability to stimulate $D^bM_{187\text{-}195}$-specific $CD8^+$ T cells. CD24 expression by adult $CD103^+$ DCs in particular has been associated with their ability to promote "lung-tropic" effector $CD8^+$ T cell responses in the lung.[26] While neonatal CD103hi DCs display a more mature scatter profile and phenotype, they retain lower expression of CD11b, CD80, CD86, and CD205 than adult $CD103^+$ DCs, indicating continued functional limitations, when compared to adult $CD103^+$ DCs. The endocytic receptor CD205 plays a role in antigen uptake and delivery for presentation on MHC Class II and cross-presentation on MHC Class I, and low CD205 expression may limit these functions for both neonatal CD103lo and CD103hi DC populations.[32] We have previously shown that following RSV infection adult mice have approximately ten times more $CD11b^+$ DCs in the MLN than neonatal mice.[25] Although fewer in number, neonatal $CD11b^+$ DCs appear nearly indistinguishable from adult $CD11b^+$ DCs. Their scatter profile and phenotype appear consistent with those of adult $CD11b^+$ DCs, with the exception of lower CD80 and CD86 expression, which may limit their ability to provide CD28-mediated costimulation.

Our functional comparison of CD103hi and CD103lo DCs in neonates aligns well with the phenotypic differences between these populations; CD103lo DCs in neonates display a lower ability to take up and process co-administered antigen. Neonatal CD103hi DCs demonstrate improvements in both of these functions, yet have lower functionality than adult $CD103^+$ DCs. It is important to note that uptake and processing are inherently linked, and measuring lower frequencies of DCs processing antigen reflects, at last in part, their limited ability to take up antigen. Despite having lower levels of antigen uptake and processing than adult $CD103^+$ DC, neonatal CD103hi DCs stimulate an "adult-like", dramatically $K^dM2_{82\text{-}90}$ -skewed $CD8^+$ T cell profile. The marked inability of CD103lo DCs to stimulate the $K^dM2_{82\text{-}90}$-specific response may be due to their limited ability to take up and process antigen and to provide costimulation, as we have previously shown that the $K^dM2_{82\text{-}90}$-specific response is more dependent on CD28-mediated costimulation than the response to $D^bM_{187\text{-}195}$.[25] The $K^dM2_{82\text{-}90}$-specific response has a lower avidity than the response to $D^bM_{187\text{-}195}$.[24,31] It is possible that lower levels of $D^bM_{187\text{-}195}$ pMHC may be required for induction, particularly in the context of dampened costimulation, and that $K^dM2_{82\text{-}90}$ presented on CD103lo DCs does not achieve the threshold level for induction of T cell proliferation.

CD103lo DCs in neonates appear to have not yet undergone the final stages of DC development. The environment of the

neonatal lung may present a restriction to these final developmental stages. GM-CSF stimulates the activation and proliferation of dendritic cells and regulates CD103 expression, and the addition of GM-CSF in the later phase (day 6) of Flt3L-derived bone marrow-derived DC promotes the expression of high levels of CD103 and increases costimulatory molecule expression.[33–36] Recently, Mayer *et al.* described a protocol to generate large numbers of CD8α-like CD103$^+$ DCs in vitro from mouse bone marrow. They demonstrated that the development of CD103$^+$ DCs in culture required a prolonged culture (15–16 days) with both Flt3L and GM-CSF, with provision of GM-CSF in both early and late phases being required to promote the differentiation and homeostasis of CD103$^+$ DCs.[33] Moreover, airway epithelium-produced GM-CSF, which is also critical for the development of alveolar macrophages in early life, spikes at birth and wanes quickly thereafter.[37] We demonstrate here that naive neonatal mice have lower expression levels of GM-CSF in the lungs than adults, and this holds true for most post-infection time points (**Figure 4**). Access to this growth factor may regulate DC development and could play a role in linking early lung development to the development of tissue-resident DCs. Interestingly, IL-3 and TGFβ, which have also been shown to enhance CD103 expression on dendritic cells,[29] are expressed more highly in the lungs of RSV-infected neonates and may play a unique role in the development of the CD103$^+$ DC subset during early life. The concerted maturation of several distinct phenotypic markers and the ability to reproduce the development of CD103$^+$ DC using Flt3L and GM-CSF *in vitro* suggests there is an overarching developmental program to coordinately regulate several pathways to achieve fully functional CD103$^+$ DCs. We are further exploring early restrictions to DC development in the neonatal lung and whether this phenomenon is unique to the lung microenvironment, or also occurs in other barrier tissues.

It is tempting to speculate about an important developmental role for CD103lo DCs in the neonatal lung. In the steady-state, CD103$^+$ DCs have been shown to play a role in the maintenance and induction of tolerance.[17,18,38,39] This function may be particularly important in neonatal mice newly experiencing a world filled with many innocuous antigens. CD103lo DCs would seem a likely population to promote tolerance given their low level of maturation and costimulatory molecule expression. Interestingly, a decreased CD103hi/CD103lo ratio in the MLN compared to the lung suggests that CD103lo DCs preferentially migrate into the MLN. Lower expression of CD103, and therefore weaker binding to E-cadherin on epithelial cells in the lung may account for this preference. Thus, approaches aimed at inducing effective immunity in the lung during early life through promoting maturation of the cDC1 population could potentially interfere with the induction of tolerance. Flt3L treatment improves the innate immune responses to RSV in neonatal mice and limit lung disease upon RSV re-exposure.[40] Yet, care should be taken to prematurely force DC maturation and upset a delicate balance, particularly at sensitive barrier sites still developing and establishing long-lasting relationships with commensal bacteria. A better understanding of both the mechanisms of neonatal CD103$^+$ DC partitioning and the biological role of the CD103lo DC population will help determine the validity of this type of approach. An alternative approach is the use of antigens to which the neonatal response is as robust as that of adults. Neonates elicit responses to the $D^bM_{187\text{-}195}$ epitope as effectively as adults, and this response is highly functional at both ages.[24] Understanding the parameters that determine age-dependent differences in the immune response will help define metrics to predict early life antigenicity and improve vaccines designed to elicit anti-pathogen immunity in young infants.

METHODS

Ethics statement. Mice used in these studies were maintained according to the guidelines of the NIH Guide to the Care and Use of Laboratory Animals. Experimental procedures had approval of the Animal Care and Use Committee of the Vaccine Research Center, National Institute of Allergy and Infectious Diseases at the National Institute of Health. Mice were housed in a facility fully accredited by the Association for Assessment and Accreditation of Laboratory Animal Care International. Animal procedures were conducted in strict accordance with all relevant federal and National Institutes of Health guidelines and regulations.

Mice, RSV infections and other treatments. Adult (8-14 week old) male and female CB6F1 mice were obtained from Jackson Labs (Bar Harbor, ME) or bred in-house. Neonatal CB6F1 mice were bred in-house, the offspring of mating BALB/c female mice with C57Bl/6 males. TCR transgenic mice were produced by NCI-Frederick Laboratory Animal Sciences Program (LASP) transgenic mouse model service and subsequently bred as heterozygotes in-house as previously described.[25] Batf3$^{-/-}$ BALB/c and C57Bl/6 mice were obtained from Jackson Labs and bred in-house to obtain both neonatal and adult Batf3-deficient hybrid mice. All mice were housed in our animal care facility at NIAID under specific pathogen-free conditions, and maintained on standard rodent chow and water supplied *ad libitum*. Neonatal mice were infected at 7 days old. Mice were anesthetized using isoflurane (3%), and infected intranasally with 2×10^6 PFU of live RSV in 10% EMEM (100 µl for adults, 25 µl for mice infected at 7 days of age). For influenza infection, neonates were infected intranasally with 25 µl of PBS containing 600 $TCID_{50}$ of influenza/PR8 using the same method. All mice were killed by lethal overdose of pentobarbital (250 mg kg^{-1}). Experiments involving co-administration of either OVA-Alexa647 or OVA-DQ (Thermo Fisher Scientific, Waltham, MA) were performed by adding 50 µg protein per mouse directly to virus preparations before intranasal administration.

Flow cytometry and cytokine analysis. Following euthanasia, MLN and/or lung tissues were harvested and processed at the indicated times post-infection as previously described.[25] In most cases, tissues from 3 to 7 mice were pooled to generate one sample. After isolation, cell preparations were stained with fluorochrome-labeled antibodies to the following cell surface markers: CD11c (N418), CD11b (M1/70), CD103 (2E7), CD8α (53-6.7), I-A/I-E (M5/114.15.2), I-Ab (AF6-120.1), CD3 (145-2C11), CD86 (GL1), CD80 (16-10A1), CD24 (M1/69), CD205 (205yekta) purchased from BD biosciences, eBioscience, or Biolegend. $K^dM2_{82\text{-}90}$ and $D^bM_{187\text{-}195}$-containing tetramers were purchased from either Beckman Coulter or MBL International. All staining was done for 20 min at 4 °C in FACS staining buffer (PBS with 1% FBS and 0.05% sodium azide). Samples were collected on an LSR-II flow cytometer and data were analyzed using FlowJo version 9.9.10. For cytokine analysis, the single left lobe of naive or infected mice was collected and snap-frozen in 2 ml of MEM supplemented with 2 mM glutamine, 10 U ml^{-1} penicillin, and 10 µg ml^{-1} streptomycin. After

thawing, lung tissue was dissociated using a GentleMACS (on program lung_02) before centrifugation to remove cellular debris. Clarified lung supernatants were sent to AssayGate (Ijamsville, MD) for analysis of cytokines using a multiplex bead-based array.

Dendritic cell: T cell coculture. Dendritic cells for DC:T cell coculture were stained using the above markers as previously described and sorted on a FACSAria.[25] $CD8^+$ T cells were isolated from splenocytes of TCR transgenic mice with T cells specific for either RSV-$K^dM2_{82\text{-}90}$ or RSV-$D^bM_{187\text{-}195}$ using a CD8α T cell isolation kit (Miltenyi), then labeled with 5μM CFSE for 5 min at room temperature followed by three washes with FBS containing media. More than 95% of $CD8^+$ T cells from $K^dM2_{82\text{-}90}$-transgenic mice are tetramer-binding, epitope-specific cells, while ~70% of $CD8^+$ T cells of $D^bM_{187\text{-}195}$-transgenic mice are tetramer-binding and epitope-specific due to recognition being mediated by the TCR beta chain paired with endogenous TCR alpha. All comparisons were made between samples set up on the same day, with the same CFSE-labeled responding cell populations. $CD8^+$ T cells of each specificity (100,000) were cocultured with FACSAria-sorted populations of $CD103^+$ DCs or $CD11b^+$ DCs (10,000) from mice infected at 7days of age or as an adults in lymphocyte media without the addition of exogenous peptide for all experiments except those presented in **Supplementary Figure S6**, where dendritic cells were pulsed with the indicated concentration of $M2_{82\text{-}90}$ peptide (SYIGSINNI) for 1 h before extensive washing before coculturing with $CD8^+$ T cells. $CD8^+$ T cells were incubated with splenocytes pulsed with 10^{-6}M cognate peptide as a positive control, or splenocytes with no peptide as a negative control. Three days later, all samples were harvested and stained with antibodies to CD8, CD3, and with ViViD (for viability) before collection on a LSRII.

Statistical analysis. Statistical analyses were performed using GraphPad prism version 6.00 for Windows, www.graphpad.com, using either a student's *t*-test, or one-way or two-way ANOVA with the indicated post-tests for multiple comparisons.

SUPPLEMENTARY MATERIAL is linked to the online version of the paper at http://www.nature.com/mi

AUTHOR CONTRIBUTIONS

T.J.R., K.M.M., E.B., and D.N. performed the experiments. T.J.R., K.M.M., and B.S.G. designed the experiments, analyzed and interpreted the data, and prepared the manuscript.

DISCLOSURE

The authors declared no conflict of interest.

Official journal of the Society for Mucosal Immunology

REFERENCES

1. Desch, A.N., Henson, P.M. & Jakubzick, C.V. Pulmonary dendritic cell development and antigen acquisition. *Immunol. Res.* **55**, 178–186 (2013).
2. Guilliams, M. *et al.* Dendritic cells, monocytes and macrophages: a unified nomenclature based on ontogeny. *Nat. Rev. Immunol.* **14**, 571–578 (2014).
3. Guilliams, M. & van de Laar, L. A Hitchhiker's guide to myeloid cell subsets: practical implementation of a novel mononuclear phagocyte classification system. *Front Immunol.* **6**, 406 (2015).
4. Schraml, B.U. & Reis e Sousa, C. Defining dendritic cells. *Curr. Opin. Immunol.* **32**, 13–20 (2015).
5. Scott, C.L., Henri, S. & Guilliams, M. Mononuclear phagocytes of the intestine, the skin, and the lung. *Immunol. Rev.* **262**, 9–24 (2014).
6. Ginhoux, F. *et al.* The origin and development of nonlymphoid tissue $CD103^+$ DCs. *J. Exp. Med.* **206**, 3115–3130 (2009).
7. Greter, M. *et al.* GM-CSF controls nonlymphoid tissue dendritic cell homeostasis but is dispensable for the differentiation of inflammatory dendritic cells. *Immunity* **36**, 1031–1046 (2012).
8. Liu, K. *et al. In vivo* analysis of dendritic cell development and homeostasis. *Science* **324**, 392–397 (2009).
9. Edelson, B.T. *et al.* Peripheral $CD103^+$ dendritic cells form a unified subset developmentally related to CD8alpha$^+$ conventional dendritic cells. *J. Exp. Med.* **207**, 823–836 (2010).
10. Hildner, K. *et al.* Batf3 deficiency reveals a critical role for CD8alpha$^+$ dendritic cells in cytotoxic T cell immunity. *Science* **322**, 1097–1100 (2008).
11. Schiavoni, G. *et al.* ICSBP is essential for the development of mouse type I interferon-producing cells and for the generation and activation of CD8alpha(+) dendritic cells. *J. Exp. Med.* **196**, 1415–1425 (2002).
12. King, I.L., Kroenke, M.A. & Segal, B.M. GM-CSF-dependent, CD103+ dermal dendritic cells play a critical role in Th effector cell differentiation after subcutaneous immunization. *J. Exp. Med.* **207**, 953–961 (2010).
13. Schlitzer, A., McGovern, N. & Ginhoux, F. Dendritic cells and monocyte-derived cells: two complementary and integrated functional systems. *Semin. Cell Dev. Biol.* **41**, 9–22 (2015).
14. Schlitzer, A. *et al.* IRF4 transcription factor-dependent $CD11b^+$ dendritic cells in human and mouse control mucosal IL-17 cytokine responses. *Immunity* **38**, 970–983 (2013).
15. Suzuki, S. *et al.* Critical roles of interferon regulatory factor 4 in CD11bhighCD8alpha- dendritic cell development. *Proc. Natl Acad. Sci. USA* **101**, 8981–8986 (2004).
16. Tamura, T. *et al.* IFN regulatory factor-4 and -8 govern dendritic cell subset development and their functional diversity. *J. Immunol.* **174**, 2573–2581 (2005).
17. Bedoui, S. *et al.* Cross-presentation of viral and self antigens by skin-derived $CD103^+$ dendritic cells. *Nat. Immunol.* **10**, 488–495 (2009).
18. Desch, A.N. *et al.* CD103+ pulmonary dendritic cells preferentially acquire and present apoptotic cell-associated antigen. *J. Exp. Med.* **208**, 1789–1797 (2011).
19. Helft, J. *et al.* Cross-presenting CD103+ dendritic cells are protected from influenza virus infection. *J. Clin. Invest.* **122**, 4037–4047 (2012).
20. Mashayekhi, M. *et al.* CD8alpha(+) dendritic cells are the critical source of interleukin-12 that controls acute infection by Toxoplasma gondii tachyzoites. *Immunity* **35**, 249–259 (2011).
21. Zelenay, S. *et al.* The dendritic cell receptor DNGR-1 controls endocytic handling of necrotic cell antigens to favor cross-priming of CTLs in virus-infected mice. *J. Clin. Invest.* **122**, 1615–1627 (2012).
22. Persson, E.K. *et al.* IRF4 transcription-factor-dependent CD103(+) CD11b(+) dendritic cells drive mucosal T helper 17 cell differentiation. *Immunity* **38**, 958–969 (2013).
23. Plantinga, M. *et al.* Conventional and monocyte-derived CD11b(+) dendritic cells initiate and maintain T helper 2 cell-mediated immunity to house dust mite allergen. *Immunity* **38**, 322–335 (2013).
24. Ruckwardt, T.J. *et al.* Neonatal CD8 T-cell hierarchy is distinct from adults and is influenced by intrinsic T cell properties in respiratory syncytial virus infected mice. *PLoS Pathog.* **7**, e1002377 (2011).
25. Ruckwardt, T.J., Malloy, A.M., Morabito, K.M. & Graham, B.S. Quantitative and qualitative deficits in neonatal lung-migratory dendritic cells impact the generation of the CD8+ T cell response. *PLoS Pathog.* **10**, e1003934 (2014).
26. Kim, T.S., Gorski, S.A., Hahn, S., Murphy, K.M. & Braciale, T.J. Distinct dendritic cell subsets dictate the fate decision between effector and memory CD8(+) T cell differentiation by a CD24-dependent mechanism. *Immunity* **40**, 400–413 (2014).
27. Montagna, G.N., Biswas, A., Hildner, K., Matuschewski, K. & Dunay, I.R. Batf3 deficiency proves the pivotal role of CD8alpha dendritic cells in protection induced by vaccination with attenuated Plasmodium sporozoites. *Parasite Immunol.* **37**, 533–543 (2015).
28. Ruckwardt, T.J. *et al.* Responses against a subdominant CD8+ T cell epitope protect against immunopathology caused by a dominant epitope. *J Immunol.* **185**, 4673–4680 (2010).
29. Sathe, P. *et al.* The acquisition of antigen cross-presentation function by newly formed dendritic cells. *J. Immunol.* **186**, 5184–5192 (2011).
30. Torti, N., Walton, S.M., Murphy, K.M. & Oxenius, A. Batf3 transcription factor-dependent DC subsets in murine CMV infection: differential impact on T-cell priming and memory inflation. *Eur. J. Immunol.* **41**, 2612–2618 (2011).

31. Liu, J. *et al.* A numerically subdominant CD8 T cell response to matrix protein of respiratory syncytial virus controls infection with limited immunopathology. *PLoS Pathog.* **12**, e1005486 (2016).
32. Shrimpton, R.E., Butler, M., Morel, A.S., Eren, E., Hue, S.S. & Ritter, M.A. CD205 (DEC-205): a recognition receptor for apoptotic and necrotic self. *Mol. Immunol.* **46**, 1229–1239 (2009).
33. Mayer, C.T. *et al.* Selective and efficient generation of functional Batf3-dependent CD103 + dendritic cells from mouse bone marrow. *Blood* **124**, 3081–3091 (2014).
34. Rosler, B. & Herold, S. Lung epithelial GM-CSF improves host defense function and epithelial repair in influenza virus pneumonia–a new therapeutic strategy?. *Mol. Cell Pediatr.* **3**, 29 (2016).
35. Unkel, B. *et al.* Alveolar epithelial cells orchestrate DC function in murine viral pneumonia. *J. Clin. Invest.* **122**, 3652–3664 (2012).
36. Zhan, Y. *et al.* GM-CSF increases cross-presentation and CD103 expression by mouse CD8($^+$) spleen dendritic cells. *Eur. J. Immunol.* **41**, 2585–2595 (2011).
37. Guilliams, M. *et al.* Alveolar macrophages develop from fetal monocytes that differentiate into long-lived cells in the first week of life via GM-CSF. *J. Exp. Med.* **210**, 1977–1992 (2013).
38. Hintzen, G. *et al.* Induction of tolerance to innocuous inhaled antigen relies on a CCR7-dependent dendritic cell-mediated antigen transport to the bronchial lymph node. *J. Immunol.* **177**, 7346–7354 (2006).
39. Semmrich, M. *et al.* Directed antigen targeting in vivo identifies a role for CD103$^+$ dendritic cells in both tolerogenic and immunogenic T-cell responses. *Mucosal Immunol.* **5**, 150–160 (2012).
40. Remot, A. *et al.* Flt3 ligand improves the innate response to respiratory syncytial virus and limits lung disease upon RSV re-exposure in neonate mice. *Eur. J. Immunol.* **46**, 874–884 (2015).